

SPARSITY-BASED MULTI-TARGET DIRECT POSITIONING ALGORITHM BASED ON JOINT-SPARSE RECOVERY

W. Ke^{1,*} and L. N. Wu²

¹School of Physics Science and Technology, Nanjing Normal University, Nanjing 210046, China

²School of Information Science and Engineering, Southeast University, Nanjing 210096, China

Abstract—The direct position determination (DPD) method can improve the location accuracy compared with the traditional two-step location methods due to omitting the intermediate procedure of estimating the measurement parameters. However, the DPD methods presented so far are significantly more complex than the two-step approach. To overcome the shortcomings of the published DPD algorithms, a novel multi-target direct localization approach is firstly proposed by exploiting the jointly sparse property in the discrete spatial domain. The main idea of this paper is that the location estimation can be obtained by finding the sparsest solution according to the predefined overcomplete basis. Furthermore, the locations of targets can be obtained from noisy signals, even if the number of targets is not known *a priori*. Experimental results demonstrate that the proposed algorithm has superior positioning accuracy to other DPD methods and improves computational efficiency greatly.

1. INTRODUCTION

Location estimation technique has received considerable attention over the past few years due to its great potential to enable different kinds of localization applications. Although Global Positioning System (GPS) has been in service for many years, it is only available in GPS-enabled devices and may encounter problems in certain urban and indoor environments due to the poor signal penetration capabilities. Therefore, the location estimation technique based on existing wireless

Received 7 November 2011, Accepted 23 January 2012, Scheduled 6 February 2012

* Corresponding author: Wei Ke (wkykw@sina.com).

infrastructures has advanced rapidly in recent years, and many location estimation algorithms [1–5] have been developed after the US Federal Commission Committee (FCC) requested that the location accuracy of the emergency calls should be within 50–300 meters [6]. The traditional approach to solve the localization problem consists of a two step procedure as shown in Fig. 1. Firstly, the signal parameters such as angle of arrival (AOA), time of arrival (TOA) and time difference of arrival (TDOA) are estimated at several base stations (BSs). Secondly, the coordinates of targets are calculated by a location center exploiting the parameters estimated in the first step. On the contrary, the DPD method shown in Fig. 2 need not estimate intermediate parameters as AOAs or TOAs. Although most localization algorithms in the open literature concentrate on the two-step method, the performance of two-step method is suboptimal in general as explained in [7–9]. The DPD algorithm was first suggested by Weiss. In his approach, each base station transfers the intercepted signals to a central processing unit where the set of positions, which best matches all the collected data simultaneously, is determined [7]. The DPD method in [8] focused on the performance of DPD in the presence of model errors for signals with known waveforms. The new localization method called cyclic DPD (CDPD) was proposed in [9], which combines the two concepts, namely, cyclostationarity property and one-step localization processing.

Although the DPD approach was originally developed for a single target, it has been extended to handle multiple emitters afterwards [10, 11]. The DPD method in [10] takes advantage of

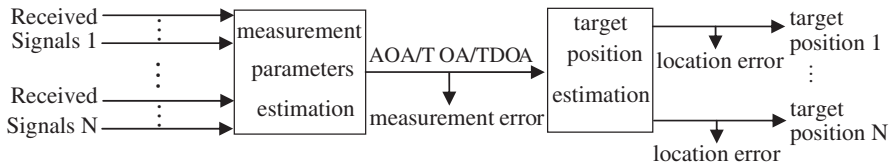


Figure 1. Basic steps of the traditional localization approach.

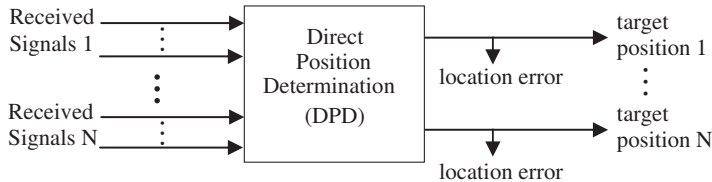


Figure 2. Basic steps of the DPD approach.

the rather simple propagation assumptions to derive the maximum likelihood (ML) estimate of the sources position. Although the algorithm resorts to a method based on the ideas of Schmidt [12] to reduce the computational complexity, a two or three dimensional grid search is also needed with high complexity. A low-complexity iterative algorithm is proposed in [11] to estimate the positions based on the ML criterion. The position of each emitter is decoupled from the other emitters, and is determined by a two dimensional grid search in each iteration. Although this approach reduces the computation load, the algorithm depends on the initial estimate of the emitters' positions. Moreover, the above algorithms cannot obtain the position estimates when the number of targets is unknown. In all these DPD approaches, the position estimates of interest are obtained directly by minimizing a cost function using the grid-search method. Therefore, the DPD methods presented so far have significantly higher complexity than the two-step approach, which can make use of the explicit geometric relationship.

In order to overcome the shortcomings of the published DPD algorithms, a novel DPD method based on the sparse representation (SR) theory [13] is considered in this paper. In fact, since the number of unknown targets is small in the discrete spatial domain at a certain time, it can be modeled as an ideal sparse vector in the localization problem. Based on this idea, a sparsity-based DPD method (SDPD) is proposed, which not only takes much less time than that of the grid-search-based DPD (GDPD) method in [10, 11], but also achieves better location performance. Furthermore, the number of targets need not be known *a priori*.

2. SIGNAL MODEL AND PROBLEM FORMULATION

Consider L transmitters and N BSs intercepting the transmitted signals. Each BS is equipped with an antenna array consisting of M elements. The bandwidth of the signal is small compared to the inverse of the propagation time over the array aperture. Denote the l th unknown target position by the vector of coordinates \mathbf{p}_l and the n th BS position by the known coordinates $\mathbf{q}_n = (x_n^B, y_n^B)$.

Although the response of possible targets could be more complex, we use the same point-target model as in [7–9], which is commonly used for source localization [14, 15] due to its simplicity. It is important to note that the point target model is not crucial to the method developed in this paper, and a more sophisticated target model could be used. Based on this model, the received signal observed by the n th BS is

given by

$$\mathbf{r}_n(t) = \sum_{l=1}^L \boldsymbol{\theta}_n(\mathbf{p}_l) s(t - \tau_n(\mathbf{p}_l)) + \mathbf{v}_n(t), \quad 0 \leq t \leq T \quad (1)$$

where $\mathbf{r}_n(t)$ is a time-dependent $M \times 1$ vector. To simplify the exposition, we only discuss the farfield scenario and confine the array to a plane, although neither of these assumptions is required for our approach. $\boldsymbol{\theta}_n(\mathbf{p}_l)$ is the n th array response to a signal transmitted from position \mathbf{p}_l . For simplicity, assume that $s(t)$ is the known signal waveform to the receivers after demodulation, e.g., training signals or synchronization signals. The propagation delay from the l th transmitter to the n th BS is given by $\tau_n(\mathbf{p}_l)$. Here, the emitters are assumed stationary or slowly moving so that the Doppler effect can be neglected. The vector $\mathbf{v}_n(t)$ represents noise and interference including model errors, which is wide-sense stationary, zero mean, complex Gaussian process, uncorrelated with the noise at the other BSs and uncorrelated with the signals. Modeling errors include calibration errors, synchronizations errors, propagation errors, etc. The length of the observation interval T is long compared with the correlation time of the signals and the correlation time of the noise processes.

Therefore, the problem discussed here can be briefly stated as follows: Given the observation signals $\{\mathbf{r}_n(t)\}_{n=1}^N$ in (1), the goal is to efficiently find the unknown locations of the transmitters as well as their number L without estimating intermediate parameters like AOA or TOAs.

3. SPARSITY-BASED DIRECT POSITIONING ALGORITHM

SR theory provides a successful framework for recovering signals that are sparse or compressible under a certain basis, with far fewer noisy measurements than the traditional methods. Exploiting the inherent sparsity in the discrete spatial domain, we develop an equivalent sparse model for multi-target direct localization.

3.1. Sparse Signal Representation

In the noisy condition, the m th element of the received vector at the k th sampling point for the n th BS is given by

$$r_n^{(m)}(k) = \sum_{l=1}^L \boldsymbol{\theta}_n^{(m)}(\mathbf{p}_l) s(t_k - \tau_n(\mathbf{p}_l)) + v_n^{(m)}(k) \triangleq \phi_n^{(m)}(k) + v_n^{(m)}(k) \quad (2)$$

Stacking the measurements of all N BSs and M array responses into a long column vector of length NM , we can obtain the equivalent measurement model at the k th sampling point as

$$\mathbf{r}(k) = \mathbf{\Phi}(\mathbf{p}) + \mathbf{v}(k) \tag{3}$$

where $\mathbf{r}(k) = [\mathbf{r}_1(k)^T, \dots, \mathbf{r}_N(k)^T]^T$ with $\mathbf{r}_n(k) = [r_n^{(0)}(k), \dots, r_n^{(M-1)}(k)]^T$; $\mathbf{\Phi}(\mathbf{p}) = [\boldsymbol{\varphi}_1(k)^T \dots \boldsymbol{\varphi}_N(k)^T]^T$ is an $NM \times 1$ matrix containing the signal waveform information and $\boldsymbol{\varphi}_n(k) = [\phi_n^{(0)}(k), \dots, \phi_n^{(M-1)}(k)]$. $\mathbf{v}(k)$ is also an $NM \times 1$ noise vector.

To cast the localization problem as a SR problem, we divide the whole plane of interest into $N_\Omega = N_x \times N_y$ grids as potential locations, and let the set of all grid location be $\Omega = \{\mathbf{p}_1^G, \dots, \mathbf{p}_{N_\Omega}^G\}$, where $\mathbf{p}_i^G = (x_i^G, y_i^G)$ is the known coordinates of the i th grid. Recognizing that the targets can occupy some such grid point, for a single time sample we are able to form a sparse location model as

$$\mathbf{r}(k) = \tilde{\mathbf{\Phi}}\boldsymbol{\alpha} + \mathbf{v}(k) \tag{4}$$

where $\tilde{\mathbf{\Phi}} = [\mathbf{\Phi}(\mathbf{p}_1^G), \dots, \mathbf{\Phi}(\mathbf{p}_{N_\Omega}^G)]$ is an $NM \times N_\Omega$ matrix representing the sparse matrix where each column is of dimensions $NM \times 1$. $\boldsymbol{\alpha}$ is an $N_\Omega \times 1$ sparse vector that having in total L nonzero entries, where the indices of nonzero entries in $\boldsymbol{\alpha}$ which represents the actual locations. Therefore, finding the actual coordinates of targets is equal to picking up the corresponding columns from the overcomplete basis. Since the location of each grid is known *a priori*, the AOA and TOA between the n th BS and the i th grid can be directly calculated according to the geometric relationship. Exploiting the known coordinates of each grid point and BS, the AOA (relative to the array baseline) of a signal emitted from \mathbf{p}_i^G to the n th BS located at \mathbf{q}_n can be calculated as $\theta_{n,i} = \tan^{-1}[(y_n^B - y_i^G)/(x_n^B - x_i^G)]$. Under a far field assumption, $\boldsymbol{\theta}_n(\mathbf{p}_i^G)$ is a function of the signal angle of arrival only. When a general uniform linear array (ULA) is considered, which will be adopted for the rest of this paper, the steering vector of n th BS takes the form

$$\boldsymbol{\theta}_n(\mathbf{p}_i^G) = [1e^{j\zeta d \cos \theta_{n,i}} \dots e^{j\zeta(M-1)d \cos \theta_{n,i}}]^T \tag{5}$$

where $\zeta = 2\pi/\lambda$ is the signal wave number, λ the wave length, and d the elements spacing. Similarly, the propagation delay between the n th BS and i th grid can be calculated as $\tau_n(\mathbf{p}_i^G) = \sqrt{(x_n^B - x_i^G)^2 + (y_n^B - y_i^G)^2}/c$, where c is the propagation speed. It should be emphasized that the above AOA and TOA are calculated directly, which differs from the conventional estimating method in two-step localization approach. As a result, $\mathbf{\Phi}(\mathbf{p}_i^G)$ for any $i \in$

$\{1, 2, \dots, N_\Omega\}$ can be predefined before the positioning procedure and does not depend on the actual target locations.

With the constraint of sparsity on $\boldsymbol{\alpha}$ (only a small subset is nonzero), the problem can be efficiently solved by SR as

$$\hat{\boldsymbol{\alpha}} = \arg \min \|\boldsymbol{\alpha}\|_1, \quad s.t. \quad \left\| \mathbf{r}(k) - \tilde{\mathbf{\Phi}}\boldsymbol{\alpha} \right\|_2 \leq \varepsilon \quad (6)$$

where $\|\cdot\|_p$ stands for the l_p norm, and ε is the error allowance in SR. During the optimization procedure, the l_2 norm constrained by ε guarantees the residual $\|\mathbf{r}(k) - \tilde{\mathbf{\Phi}}\boldsymbol{\alpha}\|_2$ to be small, whereas the l_1 norm enforces the sparsity of the estimated $\boldsymbol{\alpha}$. If there is a reliable algorithm to recover the sparse vector $\boldsymbol{\alpha}$ from $\mathbf{r}(k)$ using (6), then all but a few components of the final solution $\boldsymbol{\alpha}$ will have very small magnitudes, while a few dominant ‘‘spikes’’ in $\boldsymbol{\alpha}$ represent the actual target locations. Finally, the number of these dominant spikes gives L . Note that the equality $\mathbf{p}_i^G = \mathbf{p}_l$ may not hold exactly for any $i \in \{1, 2, \dots, N_\Omega\}$ in practice. Nevertheless, by making Ω dense enough, one can ensure $\mathbf{p}_i^G \approx \mathbf{p}_l$ closely, and the remaining model errors are absorbed in the vector $\mathbf{v}(k)$.

3.2. Sparsity-Based Direct Localization Based on Joint-sparse Recovery

In the multiple target localization, the choice of L is quite important because either adding spurious peaks or missing actual sources may cause large estimation deviation. Although several methods, such as the Akaike information criterion (AIC) or minimum description length (MDL), can estimate the L value [16, 17], the accurate number of targets is difficult to obtain in the actual location scenario. Therefore, the GDPD methods which need know the number of targets *a priori* are confined in many applications. However, even if L value is unknown, the recent research in SR has revealed that a L -sparse vector can be uniquely recovered from measurement samples when $L \leq NM/2$ [18]. Although many single-measurement algorithms have been formulated that have found utility in many different applications, most of single snapshot processing methods achieve good recovery rates only for small values of L . Apart from the limit on L , the single snapshot setting in (4) has another problem. Until now, no good algorithm can ensure sparse signal recovery in the presence of noise. Since noise is ubiquitous in practical problems, we turn to the so-called joint-sparse recovery [19, 20]. A set of vectors is called jointly sparse when its elements share a common sparsity pattern. When some snapshots are available, we can combine these snapshots to improve the

estimation performance. Therefore, the data model is extended as:

$$\mathbf{Y} = \tilde{\Phi}\mathbf{S} + \mathbf{V} \tag{7}$$

where $\mathbf{Y} = [\mathbf{r}(1), \dots, \mathbf{r}(K)]$ are multiple time samples, $\mathbf{S} = [\boldsymbol{\alpha}(1), \dots, \boldsymbol{\alpha}(K)]$, and $\mathbf{V} = [\mathbf{v}(1), \dots, \mathbf{v}(K)]$ are the corresponding sparse and noise matrixes, respectively. Here, K is the number of samples. There is an important difference between (7) and (4): Matrix \mathbf{S} is parameterized temporally and spatially, but sparsity only has to be enforced in space since the signal is not generally sparse in time. One natural approach using multiple snapshots is to exploit the joint-sparse representation characteristic, which assumes that the positions of targets keep identical among different snapshots and that the difference is only reflected on their amplitude variations.

The joint-sparse problem is often solved by calculating [20]

$$\min_{\mathbf{S} \in \mathbf{Z}} \|\mathbf{S}\|_{a,b}, \quad \mathbf{Z} := \left\{ \mathbf{S} \in \mathbf{R}^{N_\Omega \times K} : \mathbf{Y} = \tilde{\Phi}\mathbf{S} \right\} \tag{8}$$

for various combinations of a and b , where the mixed norm $\|\mathbf{S}\|_{a,b}$ is defined as

$$\|\mathbf{S}\|_{a,b} = \left(\sum_{j=1}^{N_\Omega} \sum_{i=1}^K (|\mathbf{S}[j,i]|^a)^{b/a} \right)^{1/b} \tag{9}$$

Cotter uses $a = 2, b \leq 1$ to combine multiple measurement vectors and matching pursuit (MP) to solve the joint-sparse recovery [21], while Tropp analyzes for $a = 1, b = \infty$ [22] and Eldar et al. use $a = 2, b = 1$ [23]. In [23], the sufficient conditions for joint-sparse recovery by using $a = 2$ and $b = 1$ are presented. So far, the most successful recovery algorithm for the joint-sparse problem is joint l_0 approximation (JLZA) algorithm [20], which is robust to the measurement noise and can achieve a very high recovery rate. In addition, the JLZA algorithm is fast, and the complexity of JLZA remains almost constant when sparsity increases.

Generally, we can easily have several snapshots $\mathbf{r}(k), k = 1, \dots, K$ in practice, so we choose the JLZA algorithm in the location estimation stage, and the pseudocode of which is given in Table 1. In the algorithm, $\mathbf{S}^{(i)}$ denotes the value of \mathbf{S} updated at the i th iteration. Since the choice $a = 2, b = 0$ leads to a NP-hard problem, here we follow the JLZA algorithm which approximates the mixed norm $\|\mathbf{S}\|_{2,0}$ via a sequence of Gausssian functions [20]. σ is the covariance of the Gausssian function F_σ , and we start with $\sigma = \max_i \|\mathbf{S}_{(0)}[i, :]\|_1$. The parameter β controls the tradeoff between the sparsity of the signal and the residual energy. The parameters ρ, η, γ are the controlling factors for convergence speed, and their values can be decided by numerical

Table 1. JLZA algorithm.

Initialization
1. set $\mathbf{S}^{(0)} = \tilde{\Phi}^H(\tilde{\Phi}\tilde{\Phi}^H)^{-1}\mathbf{Y}$.
2. set $\sigma = 1$ and $\rho, \eta, \gamma \in \{0, 1\}$.
repeat
3. set $\beta = 1$.
4. while $F_\sigma(\beta\zeta(\mathbf{S}^{(i)}) + (1 - \beta)\mathbf{S}^{(i)}) < F_\sigma(\mathbf{S}^{(i)})$.
$\beta = \gamma\beta$
end
5. $\mathbf{S}^{(i+1)} = \beta\zeta(\mathbf{S}^{(i)}) + (1 - \beta)\mathbf{S}^{(i)}$.
6. If $\tau^{(i)} = \ \mathbf{S}^{(i+1)} - \mathbf{S}^{(i)}\ _2 < \eta\sigma$ then $\sigma = \rho\sigma$.
Until $\sigma \leq \sigma_0$

experiments. Whenever that difference is smaller than a predefined threshold value denoted by σ_0 , we stop the algorithm.

3.3. Grid Refinement

Obviously, a dense grid can achieve fine resolution, but making the grid too dense results in large computation time. In practice, even if the positions do not fall on the grid, the DPD algorithm can approximately locate the targets. Therefore, the grid search in [10, 11] was performed in two steps: a coarse search with low resolution over the full area of interest and a fine search with high resolution near the peaks found in the coarse search. This motivates us to explore the idea that can adaptively refine the grid in order to achieve better precision. We start with a fairly coarse grid and obtain approximate spatial locations. Subsequently, we make the grid finer around the approximate source locations and refine the estimates. The algorithm is as follows.

- 1) Set $j = 0$ and create a rough grid of potential target locations $\Omega^{(j)} = \{\mathbf{p}_1^G, \dots, \mathbf{p}_{N_j}^G\}$ over the full area of interest. The grid should not be too rough in order to avoid large original bias.
- 2) Form $\tilde{\Phi}^{(j)} = [\Phi(\mathbf{p}_1^G), \dots, \Phi(\mathbf{p}_{N_j}^G)]$, where $\mathbf{p}_i^G \in \Omega^{(j)}$, $i = 1, \dots, N_j$.
- 3) Use our method in Section 3.2 to obtain the estimates of the target locations $\mathbf{p}_l^{(j)}$, $l = 1, \dots, L$, and set $j = j + 1$.
- 4) Get a refined grid $\Omega^{(j)} = \{\mathbf{p}_1^G, \dots, \mathbf{p}_{N_j}^G\}$ around the approximate target locations obtained in the last step. Here, we choose simple

equispaced grid refinement, although many different ways can refine the grid.

- 5) Return to step 2 until the grid is fine enough to meet the accuracy demand for applications.

The above idea is a very natural one, but it should be noted that if we make the grid too dense in the actual location scenario, the location errors actually increase, supported by the observations made by Donoho in [24], and Chen et al. in [25]. These articles report cases where sparsity allows one to resolve beyond the nominal Rayleigh spacing limit, but eventually the sensitivity to errors grows, depending on the number of targets within one Rayleigh spacing. Because it is not possible to make the grid infinitely fine, the SDPD method based on the JLZA algorithm cannot obtain the exact positions even if the data are noise-free. Therefore, we generally choose a suitable grid density according to the demand of applications and typically make the grid refinement only 1–2 times.

4. SIMULATION RESULTS

In order to examine the performance of the proposed SDPD method and compare it with the decoupled GDPD approach in [11] and non-decoupled GDPD approach in [10], we performed extensive Monte Carlo simulations. The location system consists of four BSs placed at coordinates (500, 500), (500, -500), (-500, 500) and (-500, -500), as shown in Fig. 3. All units are meters. The carrier frequency of the simulated signal is assumed to be 900 MHz, and its baud rate is set to be 100 kHz. Each BS is equipped with a ULA of ten antenna elements and the spacing between adjacent elements is $d = \lambda/2$. The target locations are selected at random, uniformly, within the square formed by the BSs. The signals, and the noise, are assumed as random complex Gaussian vectors with zero mean and covariance matrices $\omega_s^2 \mathbf{I}$, and $\omega_v^2 \mathbf{I}$, respectively [8–11, 26]. Our definition of signal to noise ratio (SNR) is $\text{SNR}[\text{dB}] \triangleq 10 \log_{10}(\omega_s^2/\omega_v^2)$. For a given SNR, we make 100 simulations to obtain the statistical properties of the performance. Instead of having a universally fine grid, the plane in a 1000 m \times 1000 m square was discretized in two steps: create a rough grid with 20 m resolution over the full area of interest and a fine search with 1 m resolution near the peaks found in the coarse location. Since the GDPD methods in [10, 11] need know the number of targets, the L value is estimated by the AIC or MDL method in advance. Details can be found in [16, 17], and the reference therein. In JLZA algorithm, the value of β depends on the noise level, and experimental results suggest

that $\beta = 1$ is a good choice in the beginning [20]. A wide range of numerical experiments in [20] suggests that the best setting of η is 0.5 and γ fixed to 0.5. The final value of σ_0 depends on the noise level. Numerical simulations in noisy cases suggest that $\rho = 0.1$ and $\sigma_0 = 0.001$ are good choices [20]. The experiments have been run on a Pentium IV-2.4GH processor with 1 GB memory.

4.1. RMSE Versus Number of Measurement Samples

In the first test case, the localization errors versus the number of measurement samples needed in three different algorithms are studied when SNR is set to 10dB. The number of targets is fixed at 3, and the number of measurement samples varies between 2 and 300. The localization error is defined as the average root mean square error (RMSE) between the true positions and the estimated positions of three targets, that is

$$\text{RMSE} = \frac{1}{L} \sum_{l=1}^L \sqrt{\frac{1}{J} \sum_{j=1}^J [(\hat{x}_{j,l} - x_l)^2 + (\hat{y}_{j,l} - y_l)^2]} \quad (10)$$

where J is the number of Monte Carlo simulations, and (x_l, y_l) denotes the true location of the l th target.

As the experimental results shown in Fig. 4, the localization error of the SDPD algorithm decreases sharply and becomes small as the number of measurement samples increases. About 32 samples are enough for the SDPD algorithm to achieve a high estimation accuracy, while the decoupled GDPD method need about 50 samples to get the similar precision. As for the non-decoupled GDPD algorithm, the sufficient number of measurement samples is at least 200. Moreover, with the number of measurement samples increasing, the RMSE of

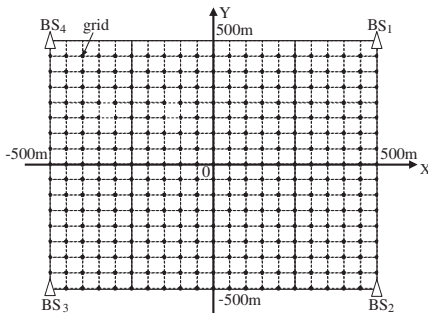


Figure 3. Simulation layout of an experiment area.

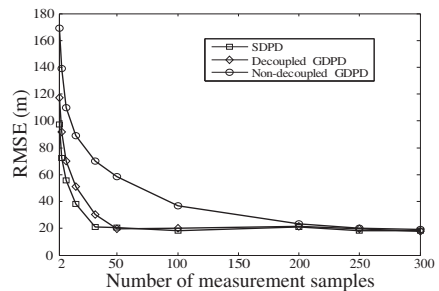


Figure 4. Effects of the number of measurement samples on the RMSE.

all three algorithms will not apparently decrease after convergence. This result shows that the SDPD algorithm based on joint-sparse representation can obtain the location estimates by using only a small number of noisy measurement samples.

4.2. RMSE Versus Number of Targets

The second simulation investigates the performance of three different DPD algorithms as a function of the number of targets. The number of targets changes from 1 to 7, and the SNR is also equal to 10 dB. According to the results from Section 4.1, the number of measurement samples is set as 32, 50 and 200 for SDPD, decoupled and non-decoupled GDPD, respectively. Fig. 5 illustrates the location error with respect to the number of targets. With the increase in the number of targets, the RMSE of two GDPD algorithms increases quickly due to the high sensitivity to the estimated number of targets. On the contrary, the variation of RMSE in the SDPD algorithm is very small. The importance of the low sensitivity of our algorithm to the number of targets is twofold. First, the number of sources is usually unknown, and low sensitivity provides robustness against mistakes in estimating the number of targets. In addition, even if the number of sources is known, low sensitivity may allow one to reduce the computational complexity.

4.3. Complexity Analysis and Comparison

To compare the computational complexity associated with the three algorithms, the simulation is conducted under the same number of measurement samples, which is set as 200 for three methods. The SNR is 10 dB as before.

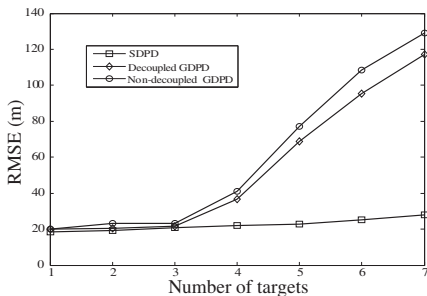


Figure 5. Effects of the number of measurement samples on the RMSE.

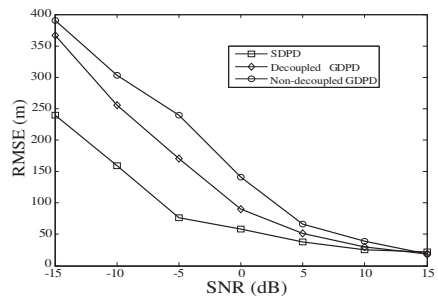


Figure 6. RMSE of three algorithms under the different SNR.

Table 2. Computer running time of the three algorithms.

Number of targets \ Algorithm	Non-decoupled GDPD	Decoupled GDPD	SDPD
2	1.019 s	0.776 s	0.266 s
3	1.553 s	1.372 s	0.267 s
4	2.263 s	1.849 s	0.271 s
5	2.751 s	2.360 s	0.273 s
6	3.669 s	3.032 s	0.276 s
7	4.441 s	3.981 s	0.279 s

Table 2 shows the complexity comparison results of the three algorithms in terms of the actual average computation time for a single run. Table 2 shows that the computer running time of the proposed method is one order less than that of two GDPD algorithms. Furthermore, with increasing the number of targets, the variation of the computer running time of the SDPD method is very small, while the computing time of two GDPD methods is monotonically increasing, because the complexity of the JLZA algorithm remains almost constant when sparsity increases.

4.4. RMSE Versus SNR

In the fourth simulation, the localization errors with respect to SNR are studied. The number of targets is fixed at 3, and the number of measurement samples is set as 32, 50 and 200 for SDPD, decoupled and non-decoupled GDPD, respectively. Here, the SNR changes from -15 dB to 15 dB. As shown in Fig. 6, we can see that the advantage of the SDPD algorithm is obvious at low SNR. Compared with the decoupled and non-decoupled GDPD algorithms, the RMSE is improved approximately 100 m to 200 m when the SNR varies from -15 dB to -5 dB. At high SNR, the performance improvement of RMSE is not very visible and all methods give the similar results. These results reveal that the SDPD method is very robust to bad propagation environments and can effectively enhance location accuracy.

5. ON-SITE EXPERIMENTAL RESULTS

To validate the performance of our algorithm in the realistic environment, a practical experiment is conducted in the campus

of Southeast University (SEU) with an area of 0.37 km^2 under the 900 MHz communication system. The measurement system uses a laptop computer, two smart phones which incorporate GPS receivers, and four HuaWei Test Mobile BSs with a lower antenna height of 3.5 m. Different from the ULA used in Section 4, here each BS is equipped with a circular array of five antenna elements, and the radius of the array is one wavelength. During the measurement phase, the mobile BSs are stationary at fixed locations. The smart phones are linked with the test BSs in dedicated test mode.

In this section, we only create a grid with 20 m resolution over the full area without grid refinement. We randomly chose 20 reference locations for each smart phone in this area and the testing data were collected, 50 samples for every location. The distance between two smart phones ranges from 50 m to 100 m. The true locations of two smart-phones, which were collected by the GPS receivers, were recorded in the smart phones to compare them with the detected locations. All measurement data were periodically stored in log files in the laptop computer. These collected experimental data were treated offline.

The performance of our algorithms was evaluated by four error measures including standard deviation of error, mean error, 67% CEP (circular error probable) and 95% CEP. The CEP is defined as the radius of the circle that has its center at the true location and contains the location estimates with a probability. Table 3 reports the error measures for different algorithms at the SEU campus. The table shows that the SDPD method provides the best positioning performance among the three algorithms. Although the decoupled GDPD approach outperforms the non-decoupled GDPD approach, the SDPD method can further improve the location accuracy. The significant improvements at mean, 67% CEP, and 95% CEP reduction are 15.1%, 21.9% and 23.2%, respectively, compared to the decoupled GDPD approach. It should also be noted that the standard deviation is obviously large in the realistic environment. The main reason is that the predefined overcomplete basis in this paper is built on the Gaussian noise assumption. In fact, our approach can achieve superior positioning performance in open regions such as the football field, where the line-of-sight (LOS) propagation probability is high and the measurement error under LOS conditions is usually considered as following the Gaussian distribution [2, 4]. However, in the multipath environment, the non-line-of-sight (NLOS) error follows the different statistical distributions in different regions, and thus the realistic signal will not match our predefined model, thereby increasing the localization errors substantially. To overcome this drawback, the

Table 3. Four error measures (in meters) for three algorithm in a realistic environment.

Algorithms	Mean \pm Standard deviation	67% CEP	95% CEP
non-decoupled GDPD	83.55 \pm 79.15	81.12	139.87
decoupled GDPD	78.63 \pm 80.69	75.66	131.15
SDPD	66.76 \pm 82.19	59.09	100.69

adaptive sensing method, such as dictionary learning technique, can be used to improve our method for recovering the sparse solution adaptively in the different environment.

6. CONCLUSION

In this paper, we investigate a formulation of the multi-target direct localization problem in the SR framework. We exploit the joint-sparse property to present a novel sparsity-based DPD algorithm as opposed to the grid-search method, thereby reducing the complexity of the DPD algorithm. At the same time, the SDPD method can further reduce the location errors compared with the GDPD algorithms. Simulation results indicate that the RMSE reduction is over 100m under the same low SNR conditions. Moreover, this algorithm can perform well with a limited number of samples and does not require any knowledge about the number of targets. This study also applies the proposed algorithm to locate multiple targets in a realistic environment. On-site experimental results demonstrate that the SDPD method outperforms the GDPD schemes, reducing the 67th and 95th percentile location errors by 21.9%–27.2% and 23.2%–28.0%, respectively, compared with the decoupled and non-decoupled GDPD algorithms. Further research will emphasize the model error analysis and the theoretic bound on the localization precision.

ACKNOWLEDGMENT

This work is supported in part by the Natural Science Foundation of the Jiangsu Higher Education Institutions of China under Grant 10KJB510008, and in part by the National High Technology Research and Development Program of China (863 Program) (2008AA01z227).

REFERENCES

1. Mitilneos, S. A. and S. C. A. Thomopoulos, "Positioning accuracy enhancement using error modeling via a polynomial approximation approach," *Progress In Electromagnetics Research*, Vol. 102, 49–64, 2010.
2. Sayed, A. H., A. Tarighat, and N. Khajehnouri, "Network-based wireless location," *IEEE Signal Processing Magazine*, Vol. 22, No. 4, 24–40, 2005.
3. Reza, A. W., S. M. Pillai, K. Dimiyati, and K. G. Tan, "A novel positioning system utilizing zigzag mobility pattern," *Progress In Electromagnetics Research*, Vol. 106, 263–278, 2010.
4. Gezici, S., "A survey on wireless position estimation," *Wireless Personal Communications*, Vol. 44, No. 3, 263–282, 2008.
5. Seow, C. K. and S. Y. Tan, "Localization of omni-directional mobile device in multipath environments," *Progress In Electromagnetics Research*, Vol. 85, 323–348, 2008.
6. FCC Docket No. 94–102, "Revision of the commission's rules to ensure compatibility with enhanced 911 emergency callin systems," RM-8143, Jul. 26, 1996.
7. Weiss, A. J., "Direct position determination of narrowband radio frequency transmitters," *IEEE Signal Processing Letters*, Vol. 11, No. 5, 513–516, 2004.
8. Amar, A. and A. J. Weiss, "Direct position determination approach in the presence of model errors-known waveforms," *Digital Signal Processing*, Vol. 16, 52–83, 2006
9. Reuven, A. M. and A. J. Weiss, "Direct position determination of cyclostationary signals," *Signal Processing*, Vol. 89, 2448–2464, 2009
10. Weiss, A. J. and A. Amar, "Direct position determination of multiple radio signals," *EURASIP Journal on Applied Signal Processing*, Vol. 2005, No. 1, 37–49, 2005.
11. Amar, A. and A. J. Weiss, "A decoupled algorithm for geolocation of multiple emitters," *Signal Processing*, Vol. 87, 2348–2359, 2007.
12. Schmidt, R. O., "Multiple emitter location and signal parameter estimation," *IEEE Transactions on Antennas and Propagation*, Vol. 34, No. 3, 276–280, 1986.
13. Donoho D., "Compressed sensing," *IEEE Transactions on Information Theory*, Vol. 52, No. 4, 1289–1306 2006.
14. Malioutov, D., M. Cetin, and A. S. Willsky, "A sparse signal reconstruction perspective for source localization with sensor

- arrays,” *IEEE Transactions on Signal Processing*, Vol. 53, No. 8, 3010–3022, 2005.
15. Zhang, Y., Q. Wan, and A.-M. Tan, “Localization of narrow band sources in the presence mutual coupling via sparse solution finding,” *Progress In Electromagnetics Research*, Vol. 86, 243–257, 2008.
 16. Wax, M. and T. Kailath, “Detection of signals by information theoretic criteria,” *IEEE Transactions on Acoustics, Speech, and Signal Processing*, Vol. 33, No. 2, 387–392, 1985.
 17. DeRidder, F., R. Pintelon, J. Schoukens, and D. P. Gillikin, “Modified AIC and MDL model selection criteria for short data records,” *IEEE Trans. on Instrument and Measurement*, Vol. 54, No. 1, 144–150, 2005.
 18. Hyder, M. M. and K. Mahata, “Direction-of-arrival estimation using a mixed $\ell_{2,0}$ norm approximation,” *IEEE Transactions on Signal Processing*, Vol. 58, No. 9, 4646–4655, 2010
 19. Cotter, S., B. Rao, K. Engan, and K. K. Delgado, “Sparse solutions to linear inverse problems with multiple measurement vectors,” *IEEE Transactions on Signal Processing*, Vol. 53, No. 7, 2477–2488, 2005.
 20. Hyder, M. M. and K. Mahata, “A robust algorithm for joint-sparse recovery,” *IEEE Signal Processing Letters*, Vol. 16, No. 12, 1091–1094, 2009.
 21. Cotter, S., “Multiple snapshot matching pursuit for direction of arrival (DOA) estimation,” *Proceedings of European Signal Processing Conference*, 247–251, Poznan, Poland, Sep. 2007.
 22. Tropp, J., “Algorithms for simultaneous sparse approximation: Part II: Convex relaxation,” *Signal Processing*, Vol. 86, 589–602, 2006
 23. Mishali, M. and Y. Eldar, “Reduce and boost: Recovering arbitrary sets of jointly sparse vectors,” *IEEE Transactions on Signal Processing*, Vol. 56, No. 10, 4692–4702, 2008.
 24. Donoho, D. L., “Superresolution via sparsity constraints,” *SIAM Journal on Mathematical Analysis*, Vol. 23, No. 5, 1309–1331, 1992.
 25. Chen, S. S., D. L. Donoho, and M. A. Saunders, “Atomic decomposition by basis pursuit,” *SIAM Journal on Scientific Computing*, Vol. 20, 33–61, 1999.
 26. Weiss, A. J., “Direct Geolocation of wideband emitters based on delay and Doppler,” *IEEE Transactions on Signal Processing*, Vol. 59, No. 6, 2513–2521, 2011.